2-18-2017

Lowest matric potential in quartz: Metadynamics evidence

Chao Zhang
Michigan Technological University

Yi Dong
Chinese Academy of Sciences

Zhen Liu
Michigan Technological University

AGU PUBLICATIONS

Geophysical Research Letters

RESEARCH LETTER
10.1002/2016GL071928

Key Points:
- A general theoretical framework is proposed to determine the lowest matric potential for soil water adsorption based on metadynamics
- The lowest matric potential of water adsorption on the quartz mineral is determined as −2.00 GPa
- In addition to the water-mineral interaction, the adsorptive water layer structure has proved to contribute to the lowest matric potential

Correspondence to:
Y. Dong,
dongyi0903@gmail.com;
ydong@mines.edu

Citation:
Zhang, C., Y. Dong, and Z. Liu (2017), Lowest matric potential in quartz: Metadynamics evidence, *Geophys. Res. Lett.*, *44*, 1706–1713, doi:10.1002/2016GL071928.

Received 11 NOV 2016
Accepted 19 JAN 2017
Accepted article online 24 JAN 2017
Published online 18 FEB 2017

Lowest matric potential in quartz: Metadynamics evidence

Chao Zhang[1], Yi Dong[2,3], and Zhen Liu[1]

[1]Department of Civil and Environmental Engineering, Michigan Technological University, Houghton, Michigan, USA, [2]Now at State Key Laboratory of Geomechanics and Geotechnical Engineering, Institute of Rock and Soil Mechanics, Chinese Academy of Sciences, Wuhan, China, [3]Formerly at Department of Civil and Environmental Engineering, Colorado School of Mines, Golden, Colorado, USA

Abstract The lowest matric potential is an important soil property characterizing the strength of retaining water molecules and a key parameter in defining a complete soil water retention curve. However, the exact value of the lowest matric potential is still unclear and cannot be measured due to the limitation of current experimental technology. In this study, a general theoretical framework based on metadynamics was proposed to determine the lowest matric potential in quartz minerals. The matric potential was derived from partial volume free energy and can be further calculated by the difference between the adsorption free energy and self-hydration free energy. Metadynamics was employed to enhance molecular dynamics for determination of the adsorption free energy. In addition to the water-mineral interaction, the adsorptive water layer structure was identified as an important mechanism that may lower the free energy of water molecules. The lowest matric potential for quartz mineral was found as low as −2.00 GPa.

1. Introduction

The total water potential in soils is defined as the total free-energy change in a unit volume of water in soil transferred reversibly and isothermally from a free-water state (i.e., pure bulk water state) to a soil water state (i.e., in soil matrix) [*Slatyer and Taylor*, 1960; *Noy-Meir and Ginzburg*, 1967]. The total water potential is an important property governing various soil behaviors, such as water migration [e.g., *Richards*, 1965; *Gardner*, 1986] and effective stress evolution [e.g., *Lu and Likos*, 2004]. There are three components contributing to the total water potential: gravitational potential, osmotic potential, and matric potential [*Iwata et al*., 1988]. Excluding the influence of elevation and solute, the total water potential is equal to the matric potential. The matric potential, as a negative of matric suction, signifies that the free energy of the soil water is lower than that of the pure bulk water. The thermodynamic energy equilibrium between the matric potential and the soil water content, which is coined in the soil water retention curve (SWRC) [e.g., *Brooks and Corey*, 1964; *van Genuchten*, 1980], characterizes a soil's pore size distribution and surface properties of its minerals [*Revil and Lu*, 2013] and quantifies the capability of the soil in retaining water at a particular energy state.

Various models have been established to describe the SWRC. Nevertheless, the lowest matric potential or the highest matric suction of a soil at complete dryness has been challenging researchers theoretically and experimentally. For instance, van Genuchten's model of SWRC [*van Genuchten*, 1980] defines a negative infinite matric potential value as the soil moisture approaches the residual water content; *Campbell and Shiozawa* [1992] and *Fredlund and Xing* [1994] set a constant value of −1.0 GPa as the lower limit for the water potential; and *Jensen et al*. [2015] modified this limit to pF = 6.9 (−778 MPa). Recently, *Lu and Khorshidi* [2015] identified the dependency of the lowest matric potential of expansive clays on the type of exchangeable cations and linearly extrapolated soil suctions from 5% relative humidity of dryness to 0, leading to various numbers ranged from −475 to −1180 MPa. On the other hand, the experimental techniques for measuring the matric potential or suction at complete dryness or zero relative humidity are not yet available in practice.

The advances in the understanding of soil water retention behaviors reveal that capillary and adsorptive water can be differentiated based on the forces applied between soil solids and water molecules in different soil water retention regimes [*Tuller and Or*, 2005; *Frydman and Baker*, 2009; *Revil and Lu*, 2013]. A typical SWRC of a silty soil presented in Figure 1 shows the measured matric potentials fitted by Lu's model of SWRC [*Lu*, 2016] with a separation of adsorptive water and capillary water. The lowest matric potential and cavitation potential were introduced as two controlling parameters to capture the starting points of adsorption and

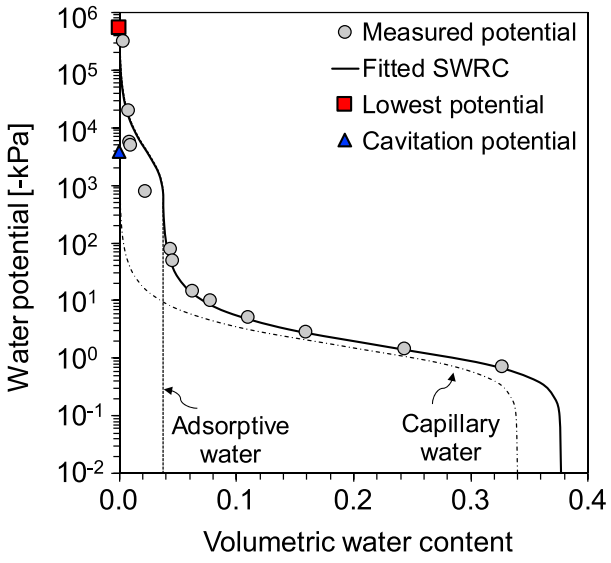

Figure 1. Typical soil water retention curve for a sandy soil (AZ1) with the separation of adsorptive water and capillary water (data from *Jensen et al.* [2015]).

capillary condensation, respectively. The lowest matric potential with a theoretical verification is still absent but is needed for a complete SWRC. When the matric potential is lower than the cavitation potential, which could range from −7 to −140 MPa where water is in a metastable state and vapor nucleation occurs [e.g., *Zheng et al.*, 1991; *Duan et al.*, 2012], adsorption mechanism dominates the soil water interactions [*Lu*, 2016]. As the water content approaches to 0, the lowest matric potential is expected to occur in the vicinity of the adsorption of the first layer of water molecules on a neutral-charged mineral surface of quartz sands.

Recently, various molecular simulation techniques have been developed to simulate solid-water interactions, such as stress states [e.g., *Luan and Robbins*, 2005; *Zhang et al.*, 2016a], phase equilibrium, and transition [e.g., *Molinero and Moore*, 2008; *Zhang et al.*, 2016b]. Among them, metadynamics [*Laio and Parrinello*, 2002] is an advanced molecular simulation technique to compute the evolution of free energy of molecular systems as a function of given variables. In this study, we first developed a general theoretical framework and then used metadynamics simulation to determine the lowest matric potential for water adsorption on a quartz mineral.

2. Methodology

2.1. Theoretical Formulation

In practice, the matric potential is usually formulated as the pressure difference between pore water (u_w) and air (u_a) at the curved air-water interface. However, it is postulated that this formulation only holds for capillary water [*Lu and Khorshidi*, 2015]. When water potential is less than the negative cavitation pressure, the concept of surface tension is not valid since the water molecules are restrained to substrates by the adsorptive forces. Therefore, a formulation of matric potential based on free-energy concepts was examined herein. The matric potential is the free-energy difference of the unit volume of water between the water retained in the soil matrix and pure bulk water. The matric potential at a particular energy state ψ (kPa or kJ/m^3) can be formulated by chemical potentials following *Noy-Meir and Ginzburg* [1967] as

$$\psi = \frac{\mu_w - \mu_w^0}{\overline{V}_w^0} = \frac{\Delta\mu_w}{\overline{V}_w^0} \tag{1}$$

where μ_w (kcal/mol) is the chemical potential of water in soils; $\mu_w{}^0$ and $\overline{V}_w^0$ are the chemical potential and molar volume of pure bulk water, respectively; and $\Delta\mu_w$ is the difference between the chemical potential of the water retained in soils and that of pure bulk water. The chemical potential of water can be calculated as [*Noy-Meir and Ginzburg*, 1967]

$$\mu_w = \left(\frac{\partial F}{\partial n_w}\right)_{X_i} \tag{2}$$

where F is the free energy, usually referred to as Gibbs free energy. For convenience, all the free energies are presented in terms of molar free energy (kcal/mole); n_w is the number of moles of water molecules under

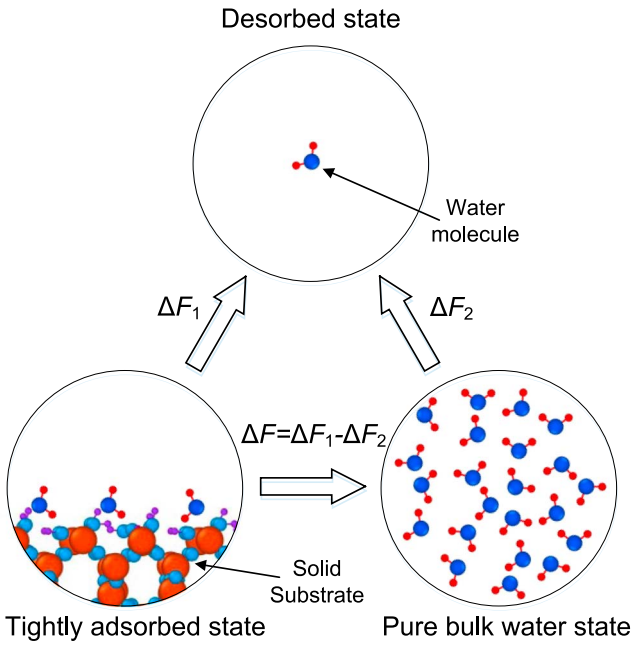

Figure 2. Schematic of different energy states and the determination of free-energy change ΔF from tightly adsorbed state to pure bulk water state.

consideration; X_i represents all other state variables (e.g., temperature and pressure) that are required constant to define the state of the system. By substituting the partial molar free energy, equation (1) can be rewritten as

$$\psi = \frac{\Delta\mu_w}{\overline{V}_w^0} = \frac{1}{\overline{V}_w^0}\left(\frac{\Delta F}{\Delta n_w}\right)_{X_i} = \left(\frac{\Delta F}{V_w^0}\right)_{X_i} \quad (3)$$

where $V_w{}^0$ is the volume of water of interest, and ΔF is the free-energy difference between soil water and pure bulk water. Note that it is difficult to determine the ΔF directly using the free energies of those two states through physical experiments or numerical simulations. Hence, a reference energy state, i.e., the desorbed state as illustrated in Figure 2, is introduced in this study to calculate the relative free energy of each state with respect to the reference state. In the desorbed state, the water molecule is assumed to be isolated in vacuum where there is no molecular interaction among water molecules. At the lowest matric potential, the soil water state corresponds to the tightly adsorbed state. The free-energy difference between the tightly adsorbed state and the desorbed state is the adsorption free energy (ΔF_1). The free-energy difference between the pure bulk water state and the desorbed state is the self-hydration free energy of pure bulk water (ΔF_2). These two free energies are frequently used in chemistry and material science [e.g., *Hermans et al.*, 1988; *Meißner et al.*, 2014]. Thereafter, ΔF can be calculated with ΔF_1 and ΔF_2:

$$\Delta F = \Delta F_1 - \Delta F_2 \quad (4)$$

The self-hydration free energy of pure bulk water (ΔF_2) has been identified as around 6.3 kcal per mole of water [e.g., *Hermans et al.*, 1988; *Jorgensen and Tirado-Rives*, 2005]. Therefore, the adsorption free energy (ΔF_1) is the only unknown variable and will be determined from the free-energy landscapes reconstructed by using the metadynamics simulation technique. This theoretical formulation is universal in thermodynamics and hence can be used to determine energy state of water or matric potential of water in soils under complex processes, such as surface adsorption, cation hydration, capillary condensation, and cavitation.

2.2. Metadynamics Simulation

The physical properties predicted by molecular dynamics simulations are reliable and useful only if the ergodic hypothesis is satisfied [*Barducci et al.*, 2011]. In other words, a sufficient simulation time scale is indispensable for a molecular system to visit all possible states of interest and then acquire authentic simulation results. In practice, due to the large number of molecules and the available computational resource, the time scale of molecular dynamics simulation is limited to several hundreds of nanoseconds to facilitate parametric investigations. This time scale may not be sufficient to output the physical properties associated with metastable states (e.g., free-energy landscapes) due to the presence of free-energy barriers [*Laio and Parrinello*, 2002]. To overcome this difficulty, metadynamics [*Laio and Parrinello*, 2002] was proposed as a powerful algorithm to enhance the sampling process by introducing additional bias potentials to some collective degrees of freedoms (also referred to as collective variables such as distances between atoms and coordination number). This technique enables the reconstruction of free-energy landscapes with acceptable time scale [*Barducci et al.*, 2011; *Laio and Gervasio*, 2008]. Metadynamics has been successfully used to reconstruct free-energy landscapes for many applications, such as adsorption process [*Meißner et al.*, 2014], solid-liquid

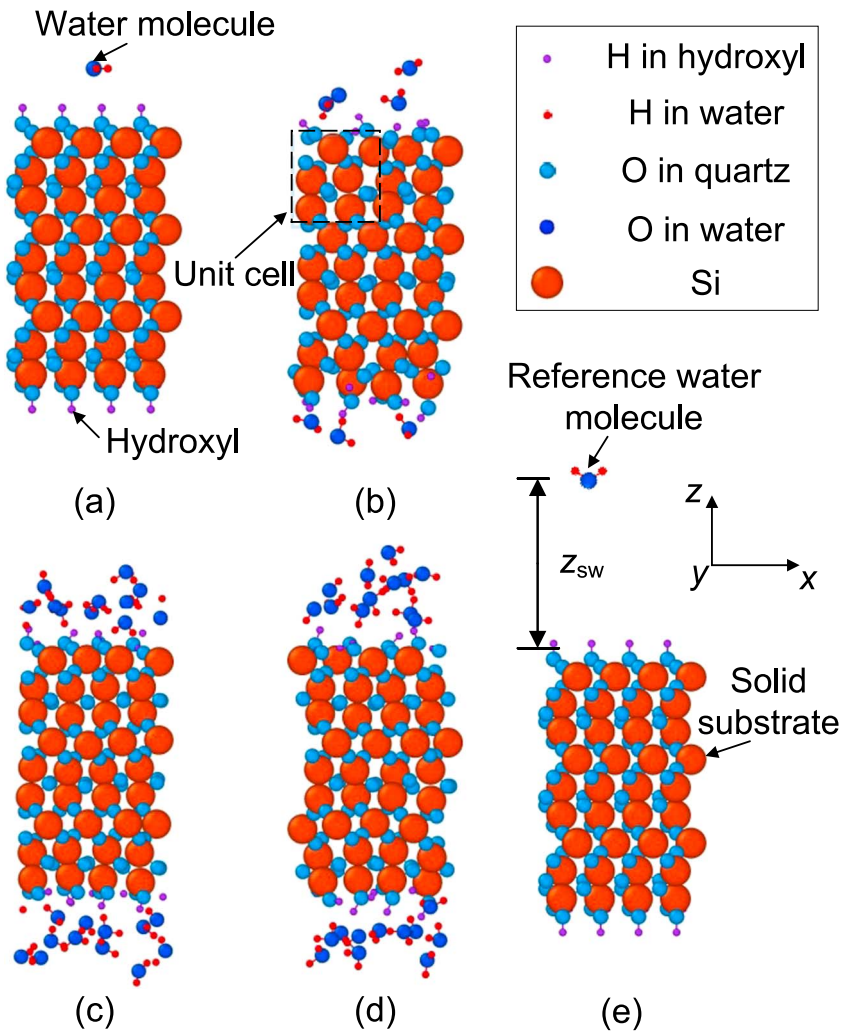

Figure 3. Snapshots of simulated water-mineral systems with different coverage of water molecules (dark blue: O in water; red: H in water; light blue: O in quartz; purple: H in hydroxyl; orange: Si): (a) 1 water molecule, (b) 4 water molecules, (c) 8 water molecules, and (d) 12 water molecules. (e) Distance of the reference water molecule from substrate z_{sw}.

interfacial energy [*Angioletti-Uberti et al.*, 2010], and protein folding [*Bussi et al.*, 2006]. In this paper, metadynamics simulation was performed in company with molecular dynamics to calculate the adsorption free energy of water in soils.

Quartz, as an uncharged substrate, is a prevalent mineral in sandy and silty types of soils [*Mitchell and Soga*, 2005]. The hydroxylated (0 0 0 1) cleavage surface of α quartz is a common stable exposed surface in nature [*Murdachaew et al.*, 2013]. Therefore, this structure was selected to calibrate the adsorption free energy of water on the quartz surface. The lattice parameters of α quartz were adopted from *Levien et al.* [1980], and the oxygen atoms on the (0 0 1) cleavage surface were replaced with hydroxyls to generate the (0 0 0 1) cleavage surface. As shown in Figure 3, water molecules were deposited on the (0 0 0 1) cleavage surface of α quartz, forming a water-mineral system for metadynamics simulations. The mineral substrate consists of $2 \times 2 \times 3 = 12$ repeating unit cells with a size of 9.832 Å × 8.515 Å × 16.216 Å. Although only four unit cells were modeled as the exposed surface, i.e., the (0 0 0 1) cleavage surface, the modeled exposed surface can be considered as infinite by introducing the periodic boundary conditions. As illustrated in Figures 3a–3d, the number of water molecules per four unit cells (N_w) deposited on the surface varies from 1, 4, 8 to 12, representing different amounts of adsorptive water.

To simulate atomistic interactions, interatomic potentials need to be defined prior to metadynamics simulations. In the water-mineral system of interest, three types of interatomic interactions were considered:

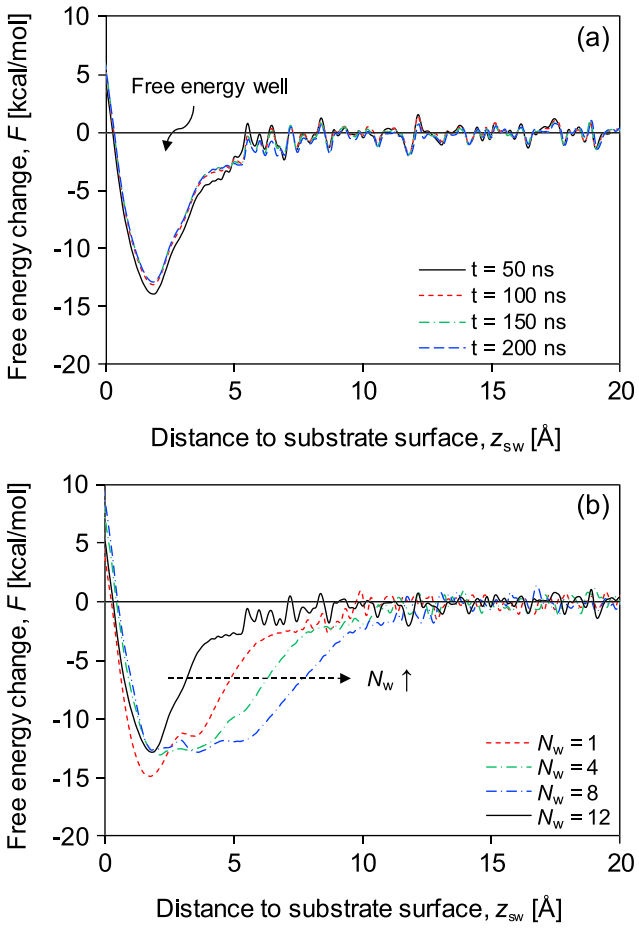

Figure 4. Adsorption free-energy landscapes: (a) comparison for $N_w = 1$ constructed with different simulation times; (b) comparison for single and multiple water molecule adsorption $N_w = 1$, 4, 8, and 12.

mineral-mineral interaction, water-mineral interaction, and water-water interaction. The former two types of interactions were calculated by the Clay Force Field (ClayFF) [*Cygan et al.*, 2004], and the water-water interaction was calculated by the 4-Point Transferable Intermolecular Potential/2005 (TIP4P/2005) water model [*Abascal and Vega*, 2005]. Therefore, the total potential energy (U_t) of the system is expressed as [*Cygan et al.*, 2004]

$$U_t = U_C + U_{vdW} + U_{bs} + U_{ab} \quad (5)$$

where U_C is the Coulombic (electrostatic) interaction energy; U_{vdW} is the short-range (van der Waals) interaction energy; U_{bs} is the bond stretch energy; and U_{ab} is the angle bend energy.

The simulation procedure includes a classical molecular dynamics stage and a subsequent metadynamics stage. At the first stage, the classical molecular dynamics simulations were performed under the canonical (NVT) ensemble using the Large-scale Atomic/Molecular Massively Parallel Simulator (LAMMPS) [*Plimpton*, 1995; *Plimpton et al.*, 2007]. Since the NVT ensemble was used, the output free energy is Helmholtz free energy rather than Gibbs free energy. However, it is postulated that Helmholtz and Gibbs free energies are approximately identical for condensed phases [*Israelachvili*, 2011]. The boundary conditions in all the directions were set as periodic. A Nosé-Hoove thermostat was employed to maintain the system temperature at $T = 300$ K. Newton's equations of motion were integrated with a time step of 1.0 fs. The short-range van der Waals interaction was calculated with a cutoff radius of 8.5 Å, and the long-range Coulombic forces were calculated using the Particle-Particle, Particle-Mesh method [*Hockney and Eastwood*, 1988] with an accuracy of 99.99%. Water molecules were kept rigid using the SHAKE algorithm [*Ryckaert et al.*, 1977]. The water-mineral systems were equilibrated at this stage for 1 ns. Next, at the second stage, the well-tempered metadynamics was performed with the PLUMED package [*Barducci et al.*, 2008; *Laio and Parrinello*, 2002; *Tribello et al.*, 2014] as a "fix" routine of LAMMPS. As illustrated in Figure 3e, the vertical distance between the mass center of the reference water molecule and the solid substrate surface (z_{sw}) was used as the collective variable to construct the adsorption free energy. Gaussian hills with a height of 1.0 kcal/mol and a width of 0.1 Å were set as the adaptive bias potentials and added to the water-mineral systems with a bias factor of 6.0 in every 1.0 ps. In this stage, metadynamics simulation was performed for 200 ns. The simulation results were visualized with the Open Visualization Tool [*Stukowski*, 2010].

3. Results and Discussions

Free-energy landscapes represented by the free-energy variation with the distance between the water molecule and substrate surface are shown in Figure 4. The sufficient time scale of the metadynamics simulation should be satisfied to ensure the convergence of the free-energy landscape simulations by varying the

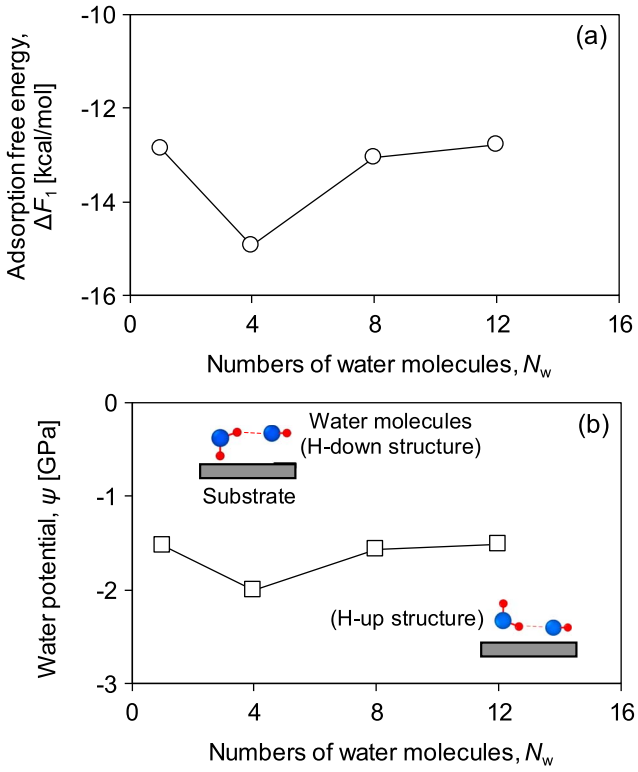

Figure 5. (a) Adsorption free energy for different coverage of water molecules. (b) Water potential for different coverage of water molecules.

simulation times (t). For this purpose, the free-energy landscapes of single water molecule adsorption with four trial simulation times are compared and presented in Figure 4a. The free-energy landscapes for time duration of 100 ns and 150 ns are more or less overlapped with each other, suggesting that 100 ns is sufficient for calculating free-energy landscape. A local free-energy minimum (−12.87 kcal/mol) around $z_{sw} = 1.85$ Å, referred to as free-energy well, indicates that 1.85 Å is the statistically stable and energetically favored position of the adsorption process and thus can be considered as reaching the tightly adsorbed state. As z_{sw} increases, the water molecule moves farther away from the surface and the free energy of the system gradually increases. This is consistent with the evolution of interaction potential between the water molecule and the mineral surface: interaction potential energy decreases as the distance increases. When z_{sw} is larger than 6 Å, the free energy is fluctuating around a constant value. This value is considered as the reference energy state, indicating that the attraction force from the mineral surface or the effect of adsorption becomes negligible. Accordingly, this reference energy state was considered as the desorbed state.

The adsorption free-energy landscapes with different numbers of water molecules per four unit cells (N_w) are presented in Figure 4b. All free-energy landscapes have similar shapes and patterns: the free energy first decreases as z_{sw} increases from 0 to 1.85 Å and then increases as z_{sw} further increases. When $z_{sw} > 15.0$ Å, the free energies in all cases start oscillating around a certain value, indicating that the interaction between the mineral surface and the reference water molecule is negligible and the reference water molecule can be considered to have reached the desorbed state. Therefore, the average free energy within $15.0 \text{ Å} < z_{sw} < 20.0$ Å was chosen as the free energy of the desorbed state. The trough forms a free-energy well representing the free-energy barrier that needs to be overcome for the tightly adsorbed state of water. In cases of multiple water molecule adsorption, the interaction among water molecules influences the adsorption free-energy landscapes and increases the width of the well as N_w increases. Specifically, as N_w increases the value of z_{sw} at which the free energy increases to zero gradually increases from 7.5 Å for $N_w = 1$, to 9.5 Å for $N_w = 4$, to 11.5 Å for $N_w = 8$, and to 14.5 Å for $N_w = 12$. The local free-energy minimum at $z_{sw} = 1.85$ Å was taken

as the free energy of the tightly adsorbed state. Then, the adsorption free energy (ΔF_1) can be calculated as the difference between the free energies of the tightly adsorbed state and desorbed state.

The adsorption free energies (ΔF_1) with different numbers of adsorptive water molecules are presented in Figure 5a. The adsorption free energy first increases and then decreases with N_w, indicating that the lowest adsorption free energy does not necessarily appear at zero water content. The adsorption free energy with $N_w = 1$ was determined as −12.87 kcal/mol, which is close to the adsorption free energy of the isolated water molecule (−12.52 kcal/mol) determined by using the density function theory [*Yang and Wang*, 2006]. Besides, the minimum adsorption free energy at $N_w = 4$ was identified as −14.92 kcal/mol, which is also consistent with the value of the H-down bilayer case (−14.99 kcal/mol) reported by *Yang and Wang* [2006]. Both cases confirm the accuracy and reliability of the adsorption free energy determined by the metadynamics simulations. The comparisons between the adsorption free energy of $N_w = 4$ and that of $N_w = 1$ implies that a more energetically favored molecular structure has been formed as the substrate adsorbs more than one water molecule. This can be further explained by the fact that different orientations of water dipoles result in different adsorptive water layer structures and thus exhibit different free energies. *Yang and Wang* [2006] found that an H-down bilayer structure in which those OH bonds point into the surface is more energetically favored than an H-up bilayer structure (OH bonds pointing up toward vacuum) as for the hydroxylated (0 0 0 1) cleavage surface of α quartz. At $N_w = 4$, the water molecules form the H-down bilayer structure and thus the minimum adsorption free energy is obtained. As the surface continues to adsorb water molecules, the adsorption free energy recovers to the same magnitude as that in the case of $N_w = 1$. Therefore, we may conclude that the adsorptive water layer structure is another factor contributing to the adsorption free energy in addition to the water-mineral interaction.

The corresponding matric potential was calculated using equation (3) with the adsorption free-energy evolution of adsorptive water molecules from 1 to 12 per four unit cells, and the results are presented in Figure 5b. The water potentials in all cases are in the same range of −1.57 GPa to −1.51 GPa, except −2.00 GPa for $N_w = 4$. These values of the lowest water potential are much lower than the numbers reported in the literature (e.g., −1.0 GPa in *Campbell and Shiozawa* [1992]). This can be explained as not only the van der Waals interaction but also the electrostatic interaction induced by polarized molecular structures on surface prevails in the adsorption of the very first few water molecules onto a mineral surface. Furthermore, since the special H-down bilayer structure of water molecules, the lowest matric potential may not occur at the exact zero water content but close to that. The above findings provide a strong and rigorous theoretical explanation and acquisition method for the lowest matric potential or the highest matric suction for water adsorbed on the quartz mineral. The proposed universal theoretical framework can be further extended to explore the adsorption of soil water by different minerals and cations, which gives sound theoretical evidence of the lowest matric potential.

4. Conclusions

This paper established a novel theoretical framework to define the lowest matric potential in SWRC model by incorporating metadynamics simulations in molecular dynamics. The matric potential is derived as partial volume free-energy difference between soil water and pure bulk water. Then, the free-energy difference is identified to be equivalent to the difference between adsorption free energy and self-hydration free energy. Metadynamics is employed to investigate the process of water adsorbed by the hydroxylated (0 0 0 1) cleavage surface of α quartz and reconstruct the corresponding adsorption free-energy landscapes. The number of water molecules per four unit cells varied from 1 to 12 to represent different coverage of water. The width of free-energy well increases with increasing number of adsorptive water molecules, indicating the increasing of the influence scope of the adsorption effect. In addition to the water-mineral interaction, the adsorptive water layer structure is an important mechanism contributing to the lowest matric potential. The lowest matric potential does not appear at exact zero water content and is determined as −2.00 GPa.

Acknowledgments
The financial support from the National Science Foundation (NSF CMMI 1562522) and the Michigan Space Grant Consortium is gratefully acknowledged. We also acknowledge Superior, a high-performance computing cluster at Michigan Technological University, for providing computational resources to fulfill this study. Data used in this study are available from the corresponding author.

References

Abascal, J. L., and C. Vega (2005), A general purpose model for the condensed phases of water: TIP4P/2005, *J. Chem. Phys.*, *123*(23), 234505.
Angioletti-Uberti, S., M. Ceriotti, P. D. Lee, and M. W. Finnis (2010), Solid-liquid interface free energy through metadynamics simulations, *Phys. Rev. B*, *81*(12), 125416.

Barducci, A., G. Bussi, and M. Parrinello (2008), Well-tempered metadynamics: A smoothly converging and tunable free-energy method, *Phys. Rev. Lett.*, *100*(2), 020603.
Barducci, A., M. Bonomi, and M. Parrinello (2011), Metadynamics, Wiley Interdisciplinary Reviews, *Comput. Molecular Sci.*, *1*(5), 826–843.
Brooks, R. H., and T. Corey (1964), Hydraulic properties of porous media, Hydrology Day Paper No. 3, Colorado State Univ., Fort Collins.
Bussi, G., F. L. Gervasio, A. Laio, and M. Parrinello (2006), Free-energy landscape for β hairpin folding from combined parallel tempering and metadynamics, *J. Am. Chem. Soc.*, *128*(41), 13,435–13,441.
Campbell, G. S., and S. Shiozawa (1992), *Prediction of Hydraulic Properties of Soils Using Particle-Size Distribution and Bulk Density Data. Indirect Methods for Estimating the Hydraulic Properties of Unsaturated Soils*, pp. 317–328, Univ. of California, Riverside.
Cygan, R. T., J. J. Liang, and A. G. Kalinichev (2004), Molecular models of hydroxide, oxyhydroxide, and clay phases and the development of a general force field, *J. Phys. Chem. B*, *108*(4), 1255–1266.
Duan, C., R. Karnik, M. C. Lu, and A. Majumdar (2012), Evaporation-induced cavitation in nanofluidic channels, *Proc. Natl. Acad. Sci. U.S.A.*, *109*(10), 3688–3693.
Fredlund, D. G., and A. Xing (1994), Equations for the soil-water characteristic curve, *Can. Geotech. J.*, *31*(4), 521–532.
Frydman, S., and R. Baker (2009), Theoretical soil-water characteristic curves based on adsorption, cavitation, and a double porosity model, *Int. J. Geomech.*, *9*(6), 250–257.
Gardner, W. H. (1986), "Water content" methods of soil analysis, in *Part 1: Physical and Mineralogical Methods*, edited by A. Klute, pp. 493–544, Soil Sci. Soc. of America, Madison.
Hermans, J., A. Pathiaseril, and A. Anderson (1988), Excess free energy of liquids from molecular dynamics simulations. Application to water models, *J. Am. Chem. Soc.*, *110*(18), 5982–5986.
Hockney, R. W., and J. W. Eastwood (1988), *Computer Simulation Using Particles*, CRC Press, New York.
Israelachvili, J. N. (2011), *Intermolecular and Surface Forces: Revised Third Edition*, Academic Press, Burlington, Mass.
Iwata, S., T. Tabuchi, and B. P. Warkentin (1988), *Soil-Water Interactions: Mechanisms and Applications*, pp. 380, Marcel Dekker Inc., New York.
Jensen, D. K., M. Tuller, L. W. de Jonge, E. Arthur, and P. Moldrup (2015), A new two-stage approach to predicting the soil water characteristic from saturation to oven-dryness, *J. Hydrol.*, *521*(2), 498–507.
Jorgensen, W. L., and J. Tirado-Rives (2005), Potential energy functions for atomic-level simulations of water and organic and biomolecular systems, *Proc. Natl. Acad. Sci. U.S.A.*, *102*(19), 6665–6670.
Laio, A., and F. L. Gervasio (2008), Metadynamics: A method to simulate rare events and reconstruct the free energy in biophysics, chemistry and material science, *Rep. Progress Phys.*, *71*(12), 126601.
Laio, A., and M. Parrinello (2002), Escaping free-energy minima, *Proc. Natl. Acad. Sci. U.S.A.*, *99*(20), 12,562–12,566.
Levien, L., C. T. Prewitt, and D. J. Weidner (1980), Structure and elastic properties of quartz at pressure, *Am. Mineral.*, *65*(9−10), 920–930.
Lu, N. (2016), Generalized soil water retention equation for adsorption and capillarity, *J. Geotech. Geoenviron. Eng.*, *142*(10), 04016051.
Lu, N., and M. Khorshidi (2015), Mechanisms for soil water retention and hysteresis at high suction range, *J. Geotech. Geoenviron. Eng.*, doi:10.1061/(ASCE)GT.1943-5606.0001325.
Lu, N., and W. J. Likos (2004), *Unsaturated Soil Mechanics*, John Wiley, Hoboken, N. J.
Luan, B., and M. O. Robbins (2005), The breakdown of continuum models for mechanical contacts, *Nature*, *435*(7044), 929–932, doi:10.1038/nature03700.
Meißner, R. H., J. Schneider, P. Schiffels, and L. Colombi Ciacchi (2014), Computational prediction of circular dichroism spectra and quantification of helicity loss upon peptide adsorption on silica, *Langmuir*, *30*(12), 3487–3494.
Mitchell, J. K., and K. Soga (2005), *Fundamentals of Soil Behavior*, John Wiley, Hoboken, N. J.
Molinero, V., and E. B. Moore (2008), Water modeled as an intermediate element between carbon and silicon, *J. Phys. Chem. B*, *113*(13), 4008–4016.
Murdachaew, G., M. P. Gaigeot, L. Halonen, and R. B. Gerber (2013), Dissociation of HCl into ions on wet hydroxylated (0001) α-quartz, *J. Phys. Chem. Lett.*, *4*(20), 3500–3507.
Noy-Meir, I., and B. Z. Ginzburg (1967), An analysis of the water potential isotherm in plant tissue. I. The theory, *Austr. J. Biol. Sci.*, *20*, 695–721.
Plimpton, S. (1995), Fast parallel algorithms for short-range molecular-dynamics, *J. Comput. Phys.*, *117*(1), 1–19.
Plimpton, S., P. Crozier, and A. Thompson (2007), *LAMMPS-Large-Scale Atomic/Molecular Massively Parallel Simulator*, vol. 18, Sandia Natl. Laboratories.
Revil, A., and N. Lu (2013), Unified water sorption and desorption isotherms for clayey porous materials, *Water Resour. Res.*, *49*, 5685–5699, doi:10.1002/wrcr.20426.
Richards, B. G. (1965), Measurement of the free energy of soil moisture by the psychrometric technique using thermistors, in *Proceedings Moisture Equilibria and Moisture Changes in Soils Beneath Covered Areas. A Symposium in Print*, edited by G. D. Aitchison, pp. 35–46, Butterworths, London.
Ryckaert, J. P., G. Ciccotti, and H. J. Berendsen (1977), Numerical integration of the cartesian equations of motion of a system with constraints: Molecular dynamics of *n*-alkanes, *J. Comput. Phys.*, *23*(3), 327–341.
Slatyer, R. O., and S. A. Taylor (1960), Terminology in plant-and soil-water relations, *Nature*, *187*(4741), 922–924.
Stukowski, A. (2010), Visualization and analysis of atomistic simulation data with OVITO–the Open Visualization Tool, *Modell. Simul. Mater. Sci. Eng.*, *18*(1), 015012.
Tribello, G. A., M. Bonomi, D. Branduardi, C. Camilloni, and G. Bussi (2014), PLUMED 2: New feathers for an old bird, *Comput. Phys. Commun.*, *185*(2), 604–613.
Tuller, M., and D. Or (2005), Water films and scaling of soil characteristic curves at low water contents, *Water Resour. Res.*, *41*, W009403, doi:10.1029/2005WR004142.
Van Genuchten, M. T. (1980), A closed-form equation for predicting the hydraulic conductivity of unsaturated soils, *Soil Sci. Soc. Am. J.*, *44*(5), 892–898.
Yang, J., and E. Wang (2006), Water adsorption on hydroxylated α-quartz (0001) surfaces: From monomer to flat bilayer, *Phys. Rev. B*, *73*(3), 035,406.
Zhang, C., Z. Liu, and P. Deng (2016a), Atomistic-scale investigation of effective stress principle of saturated porous materials by molecular dynamics, *Geophys. Res. Lett.*, *43*, 10,257–10,265, doi:10.1002/2016GL070101.
Zhang, C., Z. Liu, and P. Deng (2016b), Contact angle of soil minerals: A molecular dynamics study, *Comput. Geotech.*, *75*, 48–56.
Zheng, Q., D. J. Durben, G. H. Wolf, and C. A. Angell (1991), Liquids at large negative pressures: Water at the homogeneous nucleation limit, *Science*, *254*(5033), 829–832.